Complexation of Porphyrin with a Pyridine Moiety in Self-Assembled Monolayers on Metal Surfaces

Naoki Kanayama, Takaki Kanbara, and Hiromi Kitano*

Department of Chemical and Biochemical Engineering, Toyama University, Toyama, 930-8555 Japan

Received: March 12, 1999; In Final Form: October 21, 1999

The preparation of ordered porphyrin monolayers on the solid surfaces was pursued by noncovalent bonding. Four kinds of self-assembled monolayers (SAM) that carried pyridine moieties were constructed on the surface of silver colloids (4Py-SAM from 4,4′-dithiodipyridine, 2Py-SAM from 2,2′-dithiodipyridine, DTPA-4Py-SAM from dithiodi[*N*-(4-pyridylethyl)propylamide], and DTPA-2Py-SAM from dithiodi[*N*-(2-pyridylethyl-)propylamide]. The structure of the SAMs was observed by surface-enhanced Raman spectroscopy. When a nitrogen atom in the pyridine ring of the SAM was directed to the solution phase (in the cases of 4Py-SAM, DTPA-4Py-SAM, and DTPA-2Py-SAM), incubation of the SAM with a low concentration (<22 nM) of water-soluble porphyrin into which a zinc ion had been incorporated (zinc(II) 5,10,15,20-tetrakis(1-methylpyridinium-4-yl)porphine tetra-*p*-toluenesulfonate: TMPyP Zn(II)) resulted in a definite Raman scattering corresponding to the porphyrin ring, in addition to that of the SAM itself. In the absence of zinc ion (5,10,15,20-tetrakis(1-methylpyridinium-4-yl)-21*H*,23*H*-porphine tetra-*p*-toluenesulfonate: TMPyP H_2), on the other hand, only the scattering of the SAM was observed. Furthermore, the 2Py-SAM, in which a nitrogen atom of the pyridine ring was directed to the silver surface, showed no scattering corresponding to the porphyrin moiety, either. These results indicated that the porphyrin ring was attached to the SAM by the axial ligand linkage between the pyridine ring of the SAM and the zinc ion of the porphyrin. It was suggested that the SAM, on which porphyrin groups were fixed in the ordered manner, would be useful as molecular optical devices.

Introduction

Recently, many investigations concerning molecular recognition and molecular clusters on metal or semiconductor surfaces have been carried out for the construction of organic electrical devices which possess specific and diverse functions. Especially, organo-thin films whose structure and orientation are precisely controlled are expected to be applicable for molecular devices with a photoreactivity or a capability of molecular recognition.

Organo-sulfur compounds, such as alkyl or aromatic thiols, disulfides, and thioethers, are well-known to form close-packed and well-ordered monolayers, so-called "self-assembled monolayers" (SAMs) on the metal surfaces.[1] Since SAMs can be easily functionalized by introducing various groups, they have been extensively used as novel cell mimetic membranes or novel molecular devices. We have been trying to introduce various compounds, such as ω-mercaptoalkanoic acid,[4] polymer chains carrying many sugar residues as a pendent group,[5] cyclodextrin derivatives,[6] and phenylboronic acid derivatives,[7] onto metal surfaces as SAM and to examine their properties as novel cell mimetic membranes or as highly sensitive and specific sensing devices.

By the immobilization of porphyrin derivatives onto solid materials in a precisely controlled orientation, the network structure of the porphyrin derivatives will pursue various functions. For example, metalloporphyrins with tails of alkylmercaptan were immobilized onto the surface of a gold electrode as SAM.[8,9] Recently, it has been reported that the porphyrin was fixed onto the surface of imidazole-carrying SAM via specific axial ligands, and the further coordination of the ligands gave a multilayered structure ("sandwich" structure).[10] The multilayers of the compounds, which are abundant with π-electrons, have a strong UV-visible absorption and are expected to show a photochemical hole-burning phenomenon (PHB).[11] Using this phenomenon, memory devices and photochromic devices (the color of the materials is changed by the applied voltage)[12] can be obtained.

In this report, a self-assembled monolayer of pyridine-carrying compounds was constructed, and a metalloporphyrin derivative was attached onto the SAM as a ligand. The binding behavior of the metalloporphyrin onto the SAM was studied by using surface-enhanced resonance Raman spectroscopy (SERRS).

Experimental

Materials. 4,4′-Dithiodipyridine (4PySSPy) and 2,2′-dithiodipyridine (2PySSPy) were purchased from Tokyo Chemical Industry Co., Tokyo, Japan. Other reagents were commercially available. A Milli-Q grade water was used for preparation of sample solutions.

Syntheses of Water-Soluble Porphyrins. Zinc(II) 5,10,15,20-tetrakis(1-methylpyridinium-4-yl)porphine tetra-*p*-toluenesulfonate (TMPyP Zn(II)) and 5,10,15,20-tetrakis(1-methylpyridinium-4-yl)-21*H*, 23*H*-porphine tetra-*p*-toluenesulfonate (TMPyP H_2) were synthesized according to the method reported previously:[13] 5,10,15,20-Tetra(4-pyridyl)-21*H*,23*H*-porphyrin (TPyP) was prepared from pyridine 4-aldehyde and pyrrole. Zinc acetate dehydrate was refluxed with TPyP in a chloroform−methanol mixture (7:5) for 20 h. The product was purified by silica gel chromatography (chloroform:ethanol:pyridine = 6:1:1) (TPyP Zn(II)). TPyP Zn(II) and TPyP were refluxed with

* To whom all correspondence should be addressed. Tel.: +81−76-445−6868. Fax: +81−76-445−6703. E-mail: kitano@eng.toyama−u.ac.jp

10.1021/jp990884c CCC: $19.00
Published on Web 12/16/1999

SCHEME 1: Preparation of SAM-Forming Molecules

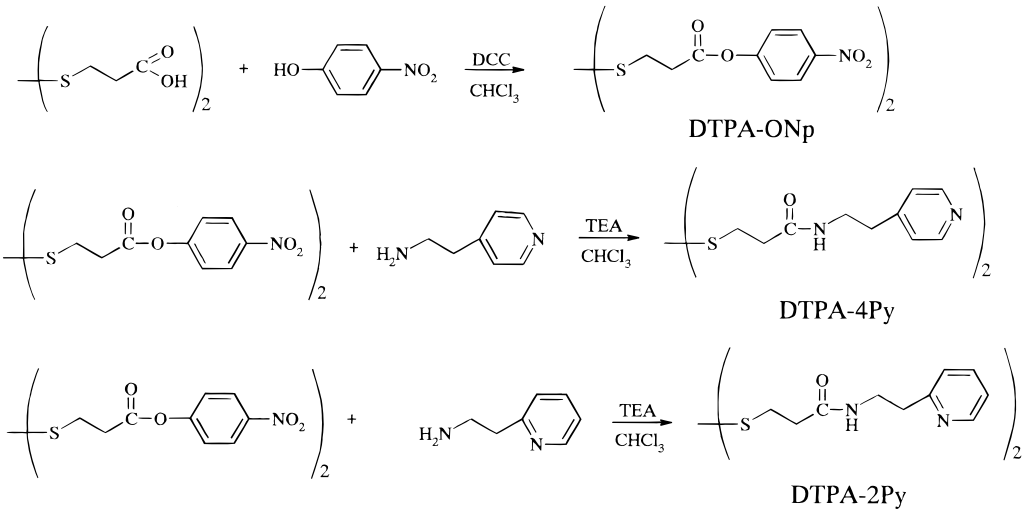

methyl *p*-toluenesulfonate for 4 h and washed with dry acetone (TMPyP Zn(II), TMPyP H_2). The concentration of water-soluble porphyrins was spectroscopically determined at a Soret band (TMPyP Zn(II): $\lambda_{max} = 437$ nm, $\epsilon_{max} = 2.04 \times 10^5$ M^{-1} cm^{-1}. TMPyP H_2: $\lambda_{max} = 422$ nm, $\epsilon_{max} = 2.30 \times 10^5$ M^{-1} cm^{-1}).

Syntheses of SAM-Forming Compounds (Scheme 1). *(1) 3,3′-Dithiodipropionic Acid Di-p-Nitrophenyl Ester (DTPA-ONp).* 3,3′-Dithiodipropionic acid (2.0 g, 9.5 mmol) dissolved in a dry chloroform (30 mL) was mixed with *p*-nitrophenol (5.29 g, 38 mmol) under stirring. *N*,*N*′-Dicyclohexylcarbodiimide (DCC, 5.88 g, 28.5 mmol) dissolved in 15 mL of dry chloroform was slowly added to the solution at room temperature. The coupling reaction was followed by TLC (silica gel plate; solvent, chloroform; R_f of the product, 0.5). One day later, white precipitates (mainly composed of DCU) were removed by filtration, and the filtrate was recovered. The precipitates were washed with dry chloroform, and the chloroform solution was added to the filtrate. The filtrate was washed with pure water, dehydrated with anhydrous Na_2SO_4, and evaporated. An oily product was precipitated by ether. The crude product was purified by silica gel chromatography (mobile phase, chloroform), and the product was recrystallized from chloroform/ether three times to give white crystals (1.78 g, 3.9 mmol, yield 41%). Anal. Calcd for $C_{18}H_{16}O_8N_2S_2$: C, 47.79; H, 3.53; N, 6.19. Found: C, 47.33; H, 3.44; N, 6.01. ^{1}H NMR (400 MHz in $CDCl_3$) δ 3.08 (m, 8H, $-CH_2-$), 7.30 (m, 4H, phenyl), 8.27 (m, 4H, phenyl). IR (KBr): ν_{arom}(C−H) 3035 cm^{-1}, ν_{as}(C−H) 2929 cm^{-1}, ν_s(C−H) 2851 cm^{-1}, ν_{as}(N═O) 1536 cm^{-1}, ν(C═C) ring 1449 cm^{-1}, ν_s(N═O) 1311 cm^{-1}, δ(C−N) 893 cm^{-1}, γ_{arom}(C−H) 641 cm^{-1}.

(2) Dithiodi[N-(4-pyridylethyl)propylamide] (DTPA-4Py) and Dithiodi[N-(2-pyridylethyl)propylamide] (DTPA-2Py). DTPA-ONp (300 mg, 0.66 mmol) dissolved in a dry chloroform (15 mL) was mixed with 4-aminoethylpyridine (425 mg, 1.73 mmol) and triethylamine (500 μL, 3.6 mmol). The reacting solution turned yellow, and after 15 h, the spot of DTPA-ONp completely disappeared in TLC. The reacting solution was washed with a saturated aqueous sodium bicarbonate and water and dried over anhydrous sodium sulfate. The organic phase was evaporated and precipitated from ether. The crude product was recrystallized three times from chloroform/ether (DTPA-4Py, 197 mg, 0.47 mmol, yield 71%). Anal. Calcd for $C_{20}H_{26}O_2N_4S_2$: C, 57.39; H, 6.26; N, 13.38. Found: C, 57.01; H, 6.30; N, 13.21. ^{1}H NMR (400 MHz in $CDCl_3$) δ 2.49 (t, 4H, $-CH_2-$), 2.85 (t, 4H, $-CH_2-$), 2.91 (t, 4H, $-CH_2-$), 3.56 (q, 4H, $-CH_2-$), 6.22 (s, 2H, −C(═O)−NH−), 7.14 (m, 4H, pyridyl), 8.48 (m, 4H, pyridyl). IR (KBr): ν(N−H) 3436 cm^{-1}, ν_{arom}(C−H) 3058 cm^{-1}, ν(C−H) 2934 and 2832 cm^{-1}, ν(C═O) amide I 1643 cm^{-1}, ν(C═C) ring 1604 cm^{-1}, δ(N−H) amide II 1552 cm^{-1}, ν(C═C) ring 1420 cm^{-1}, γ_{arom}(C−H) 813 cm^{-1}.

Using a similar procedure, DTPA-2Py was synthesized (124 mg, 0.29 mmol, yield 44%). Anal. Calcd for $C_{20}H_{26}O_2N_4S_2$: C, 57.39; H, 6.26; N, 13.38. Found: C, 57.21; H, 6.30; N, 13.30. ^{1}H NMR (400 MHz in $CDCl_3$) δ 2.54 (t, 4H, $-CH_2-$), 2.93 (t, 4H, $-CH_2-$), 2.99 (t, 4H, $-CH_2-$), 3.67 (q, 4H, $-CH_2-$), 6.79 (s, 2H, −C(═O)NH−), 7.16 (m, 4H, pyridyl), 7.61 (m, 2H, pyridyl), 8.52 (m, 2H, pyridyl). IR (KBr): ν(N−H) 3437 cm^{-1}, ν_{arom}(C−H) 3067 and 3008 cm^{-1}, ν(C−H) 2928 and 2852 cm^{-1}, ν(C═O) amide I 1640 cm^{-1}, ν(C═C) ring 1592 cm^{-1}, δ(N−H) amide II 1542 cm^{-1}, ν(C═C) ring 1475 and 1438 cm^{-1}, γ_{arom}(C−H) 760 cm^{-1}.

Preparation of Silver Colloids. Silver colloid was prepared by the reduction of $AgNO_3$ (6 mg) with $NaBH_4$ (10 mg) in water (100 mL) at 0 °C, as previously reported.[6a,b] The concentration of silver colloid was evaluated to be 360 μM by conductometric titration with a 1.0×10^{-3} M HNO_3 aqueous solution. The average hydrodynamic diameter of silver colloid was obtained to be 39.6 ± 5.8 nm by the dynamic light scattering (DLS) technique (DLS-7000, Otsuka Electronics, Hirakata, Osaka, Japan; light source, He−Ne laser 632.8 nm). UV−vis, $\lambda_{max} =$ 395 nm.

Preparation of Silver Colloid Covered with SAM. The SAM-forming compound was dissolved in H_2O (1 mM, 2 μL), added to the colloidal Ag (500 μL), and incubated for 1 h at room temperature (Scheme 2).

Raman Scattering Measurements. The Raman spectra were recorded on a Raman spectrophotometer (NR-1100, Japan Spectroscopic Co., Tokyo, Japan; light source, Ar laser 488.0 nm) with a band resolution of 5 cm^{-1} in a sealed glass capillary cell. The observation cells were thermostated by a Peltier device (Model RT-IC, Japan Spectroscopic Co.). Typical energy of the excitation laser beam was 200 mW.

Electrochemical Measurements. Cyclic voltammetric (CV) measurements were performed with a potentiostat (HA-301, Hokuto-Denko, Tokyo, Japan) and function generator (HA-104, Hokuto-Denko). Outputs of the potentiostat were converted by an A/D converter and collected by a microcomputer (PC486SE, Epson, Suwa, Japan). Data analyses were carried out with a homemade program. Gold and Pt electrodes and a KCl saturated calomel electrode (SCE) were used as working, counter, and

SCHEME 2: Chemical Structure of SAMs Carrying the Pyridine Moiety [(a) 4Py-SAM, (b) 2Py-SAM, (c) DTPA-4Py-SAM, and (d) DTPA-2Py-SAM]

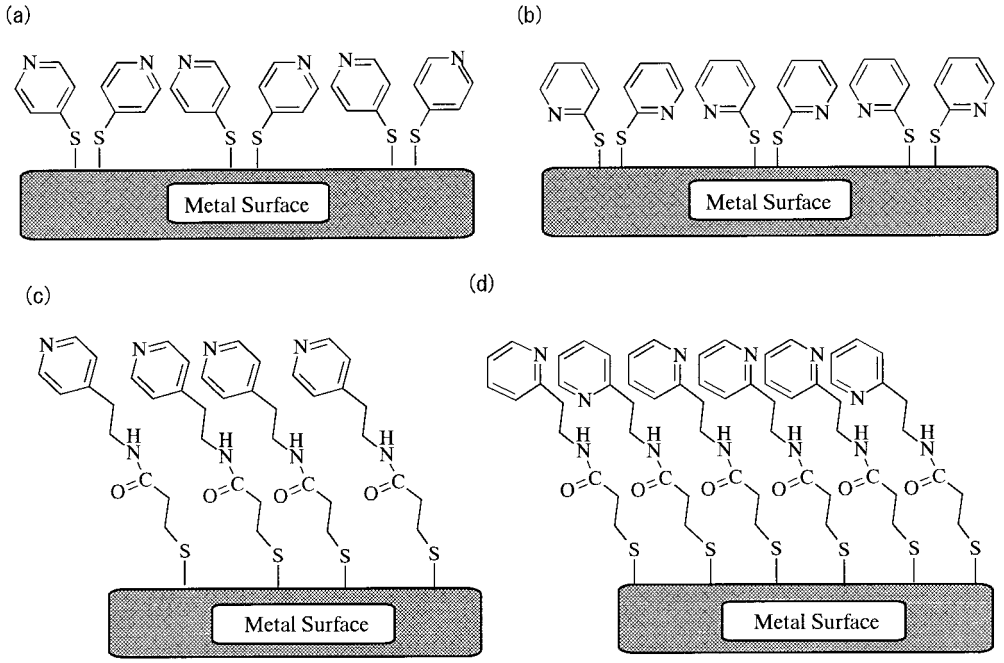

reference electrodes, respectively. An electrochemical cell was thermostated at 25 °C by a circulating water bath (RM6, Lauda, Postfach, Germany). A poly-crystalline gold electrode (geometric area, 0.020 cm^2) from BAS (Tokyo, Japan) was incubated with a solution of SAM-forming molecule (1 mM) for 24 h and rinsed with water and ethanol several times before the voltammetric experiment. The electrochemical reductive desorption of SAMs from the electrode was performed in a 0.5 M KOH aqueous solution at a scan rate of 100 mV/s.[14] The corresponding process is represented by the following equation:

$$R{-}S{-}Au + e^- = Au + R{-}S^- \qquad (1)$$

Infrared Reflection−Absorption Spectroscopy (IR−RAS) Measurements. The SAMs carrying the pyridine ring moiety were prepared by immersing the gold-evaporated substrate (Nippon Laser Electronics Co., Nagoya, Japan) in a solution of a SAM-forming molecule (1 mM) for 24 h and rinsing with water and ethanol several times. The SAM-modified gold-evaporated substrates were used for the infrared reflection−absorption spectroscopy (IR−RAS) measurements. The IR−RAS spectra of SAM were recorded on a System 2000 FT-IR (Perkin-Elmer) with an MCT detector. All IR−RAS spectra were obtained by 1024 scans at 16 cm^{-1} resolution, with a light incident on the gold substrate at 80°.

Results and Discussion

A. Characterization of SAMs of Pyridine Derivatives on Metal Surfaces. *(1) Raman Scattering Measurements of SAMs. 4Py-SAM and 2Py-SAM.* Figure 1a shows a Raman spectrum of 4PySSPy in the solid state. There was a distinct peak attributable to the disulfide group of 4PySSPy at 550 cm^{-1}. After incubation of 4PySSPy with the silver colloid, on the other hand, a Raman spectrum of the dispersion mixture showed no peak at 550 cm^{-1}, whereas a peak at 1090 cm^{-1}, corresponding to a stretching vibration of a C−S bond with aromatic ring (ν_{arom}(C−S)), became much larger than that in the solid state due to the

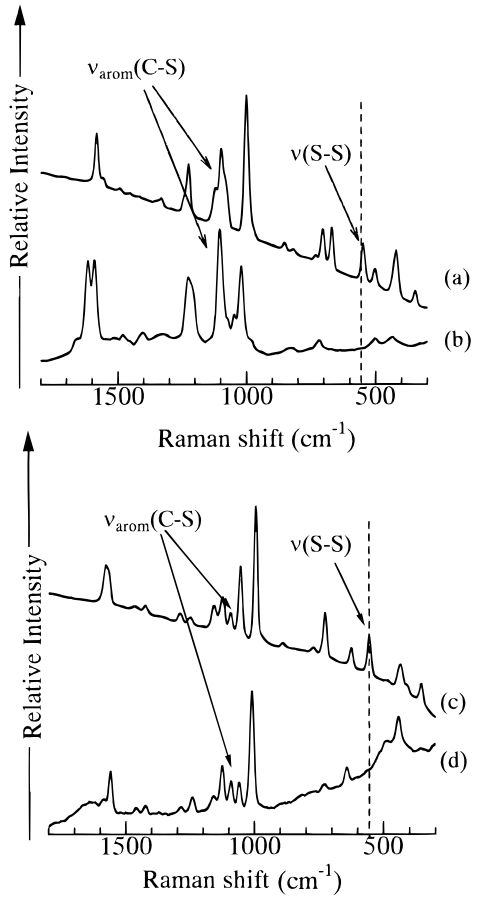

Figure 1. Raman and SERS spectra of 4PySSPy and 2PySSPy excited at 488.0 nm and 25 °C. 4PySSPy: (a) bulk solid and (b) SAM adsorbed on colloidal Ag. 2PySSPy: (c) bulk solid and (d) SAM adsorbed on colloidal Ag.

so-called "surface-enhanced Raman (SER) effect" (Figure 1b).[15] The SER effect appeared because of the formation of a Ag−S linkage (chemical effect) in the neighborhood of metal surfaces (electromagnetic effect). It should be mentioned here that the

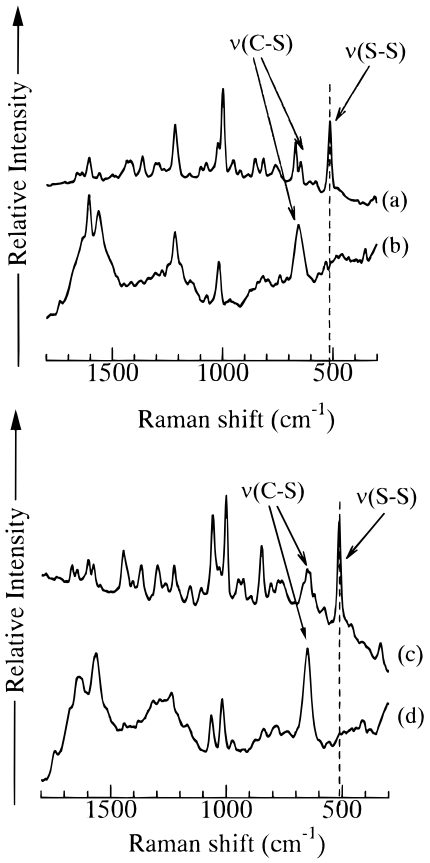

Figure 2. Raman and SERS spectra of DTPA-4Py and DTPA-2Py excited at 488.0 nm and 25 °C. DTPA-4Py: (a) bulk solid and (b) SAM adsorbed on colloidal Ag. DTPA-2Py: (c) bulk solid and (d) SAM adsorbed on colloidal Ag.

concentration of 4PySSPy in the dispersion (4 μM) was too low to be detected without the SER effect.

When the SAM is formed on the metal surface, the C−S bond exists in the closest neighborhood of the metal surface. Since the intensities of Raman scattering by molecular moieties neighboring the metal surface are most largely enhanced by the SER effect, the C−S band should be most clearly observed in comparison with other bands. Figure 1b is consistent with this explanation and indicates that the SAM was formed on the silver colloid by the cleavage of disulfide linkage. In addition, the disappearance of the ν(S−S) band definitely supported the theory that the surfaces were not coated with a multilayer of physically absorbed molecules but only with a monolayer of molecules chemically absorbed via a Ag−S bond. The formation of a SAM of 2PySSPy on the silver colloid was confirmed from both the disappearance of the disulfide band and the SER effect of the C−S bands (Figure 1c,d).

DTPA-4Py-SAM and DTPA-2Py-SAM. Figure 2a shows a Raman spectrum of DTPA-4Py in the solid state. A distinct peak attributable to the disulfide group of DTPA-4Py at 510 cm^{-1} disappeared after incubation of DTPA-4Py with the silver colloid, whereas a peak at 673 cm^{-1} corresponding to a stretching vibration of C−S bond (ν(C−S)) became much larger than that in the solid state (Figure 2b) due to the SER effect described above. In addition, after incubation of DTPA-4Py with the silver colloid, a stretching vibration of the C−S bond shifted from 673 to 660 cm^{-1}, which can be attributed to the formation of a Ag−S linkage,[16] supporting the formation of SAM on the surface of silver colloids. Similarly, the formation of a SAM of DTPA-2Py on the silver colloid was also confirmed (Figure 2c,d).

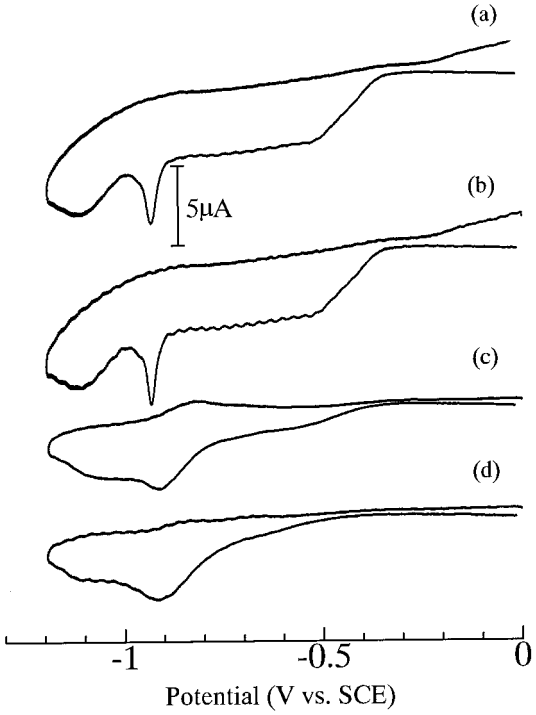

Figure 3. Voltammetric response of reductive desorption of pyridine ring-carrying SAMs in a 0.5 M KOH on the Au electrode. Scan rate, 100 mV/s. (a) 4Py-SAM, (b) 2Py-SAM, (c) DTPA-4Py-SAM, and (d) DTPA-2Py-SAM.

TABLE 1: Molecular Surface Area of Pyridine-Ring Carrying SAMs

SAM	Γ (nm^2)
4Py-SAM	0.34
2Py-SAM	0.33
DTPA-4Py-SAM	0.41
DTPA-2Py-SAM	0.27

(2) Cyclic Voltammetric Measurements of SAMs Carrying a Pyridine Moiety. The CV technique was used for the estimation of the surface area of SAM-forming molecules. The gold electrode that had been incubated with a solution of four kinds of SAM-forming compounds beforehand showed a peak at about −0.9 V by scanning from 0 to −1.2 V in a 0.5 M KOH solution (Figure 3). This peak has been attributed to the reductive desorption of thiolated compounds chemi-sorbed to Au (eq 1).[14] These results support the observation that four kinds of molecules (4PySSPy, 2PySSPy, DTPA-4Py, DTPA-2Py) could be adsorbed to the gold electrode with the cleavage of the S−S bond and following Au−S bond formation.

Using the peak area of reductive desorption curve, the molecular surface area (Γ) of SAM-forming compounds was determined (Table 1). The table shows that the compounds prepared here formed densely packed SAMs. The structure of 4Py-SAM deposited on the gold plate was previously studied by using STM.[17] The distance between the paralleled arrays of pyridine rings in the SAM was estimated to be 0.49 nm, whereas the distance between the centers of neighboring pyridine rings in each array was 1.49 nm. It was also reported previously that the surface excesses of both 4Py-SAM and 2Py-SAM on Au(100) were ca. 7×10^{-10} mol cm^{-2} and equal to each other.[18]

The Γ values for the 4Py-SAM and 2Py-SAM evaluated here were 0.34 nm^2 and 0.33 nm^2, respectively, and approximately equal each other. These values were, however, larger than that previously reported for the pyridine ring (molecular surface area = 0.24 nm^2).[18] The previous study on monolayers of alkanethi-

olates on Au(111) surfaces showed that the symmetry of sulfur atoms is hexagonal with a S−S spacing of 0.49 nm and area per molecule of 0.21 nm^2.[19] Taking account of these values, the Γ value previously reported for the pyridine ring (0.24 nm^2)[18] seems to be too small. Around the reductive desorption peak, a small and broad indefinite peak existed (Figure 2 in ref 18), which might make the reductive desorption peak area larger and result in the smaller molecular surface area.

The Γ values for the DTPA-4Py-SAM and DTPA-2Py-SAM were estimated to be 0.41 nm^2 and 0.27 nm^2, respectively. In the case of DTPA-2Py-SAM, the hydrogen bond between a nitrogen atom of the pyridine ring and the amide bond can be formed to make the neighboring DTPA-2Py moieties attract each other. Consequently, DTPA-2Py would form an ordered and well-packed SAM on a gold surface (Scheme 3). The Corey−Pauling−Koltun (CPK) model of the SAM supported this idea. In the case of DTPA-4Py-SAM, on the other hand, the hydrogen bond cannot be formed, resulting in a nonordered and less-packed SAM.

To confirm the presence of a hydrogen bond between a nitrogen atom of the pyridine ring and the amide bond moiety in the DTPA-2Py-SAM on the gold electrode, the DTPA-2Py-SAM was prepared in the solution of DTPA-2Py (1 mM) containing 4 M of urea, which is well-known to inhibit the formation of hydrogen bonds.[20] After rinsing the electrode with water and ethanol several times, the electrochemical reductive desorption of DTPA-2Py-SAM from the electrode was performed. The Γ value for the SAM prepared in the urea solution was estimated to be 0.37 nm^2, which is larger than that for DTPA-2Py-SAM shown in Table 1 (0.27 nm^2). This result suggests the presence of a hydrogen bond between the pyridine ring and the amide bond moiety. In the presence of urea, the formation of the hydrogen bond between the pyridine ring and the amide bond moiety was inhibited, and consequently, the less packed SAM was formed on the gold electrode, resulting in the increase in the Γ value.

In addition, IR−RAS measurements of the SAMs (DTPA-4Py-SAM, DTPA-2Py-SAM) were performed. The IR−RAS spectrum of DTPA-4Py-SAM showed an amide II band (ν(N−H)) at 1552 cm^{-1}, whereas that of DTPA-2Py-SAM showed the band at 1597 cm^{-1}. The blue shift of the amide II band of DTPA-2Py-SAM is due to the formation of the hydrogen bond between the pyridine ring and the amide bond moiety.[21] From both the urea-induced increase in the Γ value and the blue shift of the amide II band in the IR−RAS spectra, we could confirm the formation of a hydrogen bond between the pyridine ring and the amide moiety in the DTPA-2Py-SAM.

We tried to use a silver electrode to evaluate the Γ value of the SAM-forming compounds on the same substrate as that in the colloidal system. However, the evaluation on the Ag electrode could not be made due to a large undefined reduction peak around −1.0 V. Because of a difference between the tilt angle of the SAM-forming molecules formed on the Ag surface and that on the Au surface,[16(a),22] the Γ value of SAM-forming molecules on the Au surface must be different from that on the Ag surface. Even so, there might be the same tendency in the magnitude of molecular surface area on Ag and Au surfaces. As a result, the DTPA-2Py-SAM might be more densely packed than the DTPA-4Py-SAM in the silver colloid system, too.

B. Binding of Porphyrin to Pyridine-Carrying SAMs. *(1) TMPyP H_2/Pyridine Ring-Carrying SAM System.* Various concentrations (0−20 nM) of TMPyP H_2 without a metal ion in the core of the porphyrin were incubated with the Ag colloid dispersion, which had been incubated with the pyridine ring-carrying compounds beforehand (DTPA-4Py-SAM, DTPA-2Py-SAM, 4Py-SAM, and 2Py-SAM). After 30 min, the Raman spectra of these solutions showed no change compared with the SERS spectra of SAMs itself (data not shown), which suggests that TMPyP H_2 did not interact with the pyridine ring-carrying SAMs on colloidal Ag at all.

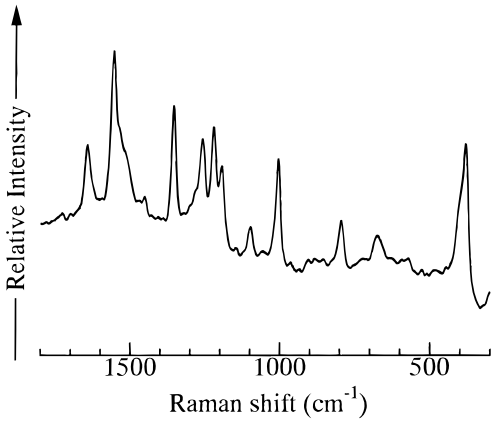

Figure 4. Raman spectrum of TMPyP Zn(II) aqueous solution excited at 488.0 nm and 25 °C. [TMPyP Zn(II)] = 5.47 × 10^{-4} M.

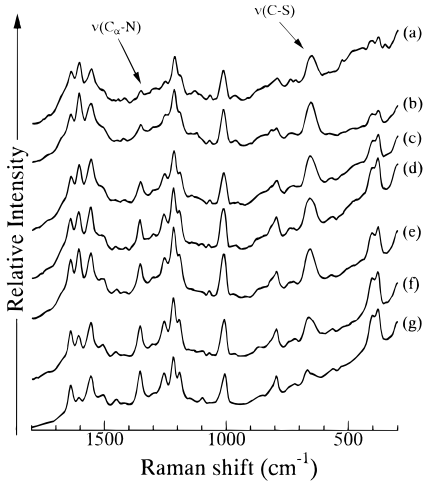

Figure 5. SERRS spectra of TMPyP Zn(II) adsorbed on a SAM of DTPA-4Py at 25 °C. Excitation wavelength, 488.0 nm. [TMPyP Zn(II)] = (a) 2.1, (b) 3.0, (c) 4.3, (d) 5.0, (e) 7.5, (f) 11, and (g) 22 nM.

(2) TMPyP Zn(II)/DTPA-4Py-SAM and 4Py-SAM Systems. The Raman spectra of DTPA-4Py-SAM, which was formed by the incubation of the Ag colloid with various concentrations of TMPyP Zn(II) (0 M−22 nM) for 30 min at room temperature, are shown in Figure 5. In this concentration range, the resonance Raman scattering of porphyrin derivatives in the bulk phase was negligible. The newly appeared bands (380, 793, 1250, and 1353 cm^{-1}) could be assigned to the Raman scattering of porphyrin. The spectral changes, therefore, could be attributed to the overlap of Raman scattering of the SAM on that of the porphyrin group, which was induced by the attachment of porphyrin group to the surface of SAM above the silver colloids (Scheme 3). The changes in the peak intensities could be solely ascribed to the summation of common linkages in the SAM and porphyrin.

The relative peak intensity of $\nu(C_\alpha\text{-N})$ between an α-carbon and a nitrogen of pyrrole in the porphyrin at 1353 cm^{-1} to that for ν(C−S) (658 cm^{-1}) was plotted against the concentration of porphyrin added (Figure 6, open circle). We assumed here that the structure and Raman spectrum of the SAM itself did not change with the binding of porphyrin. With the increase in

SCHEME 3: Adsorption of Water-Soluble Porphyrin on the Surface of SAMs Carrying the Pyridine Moiety

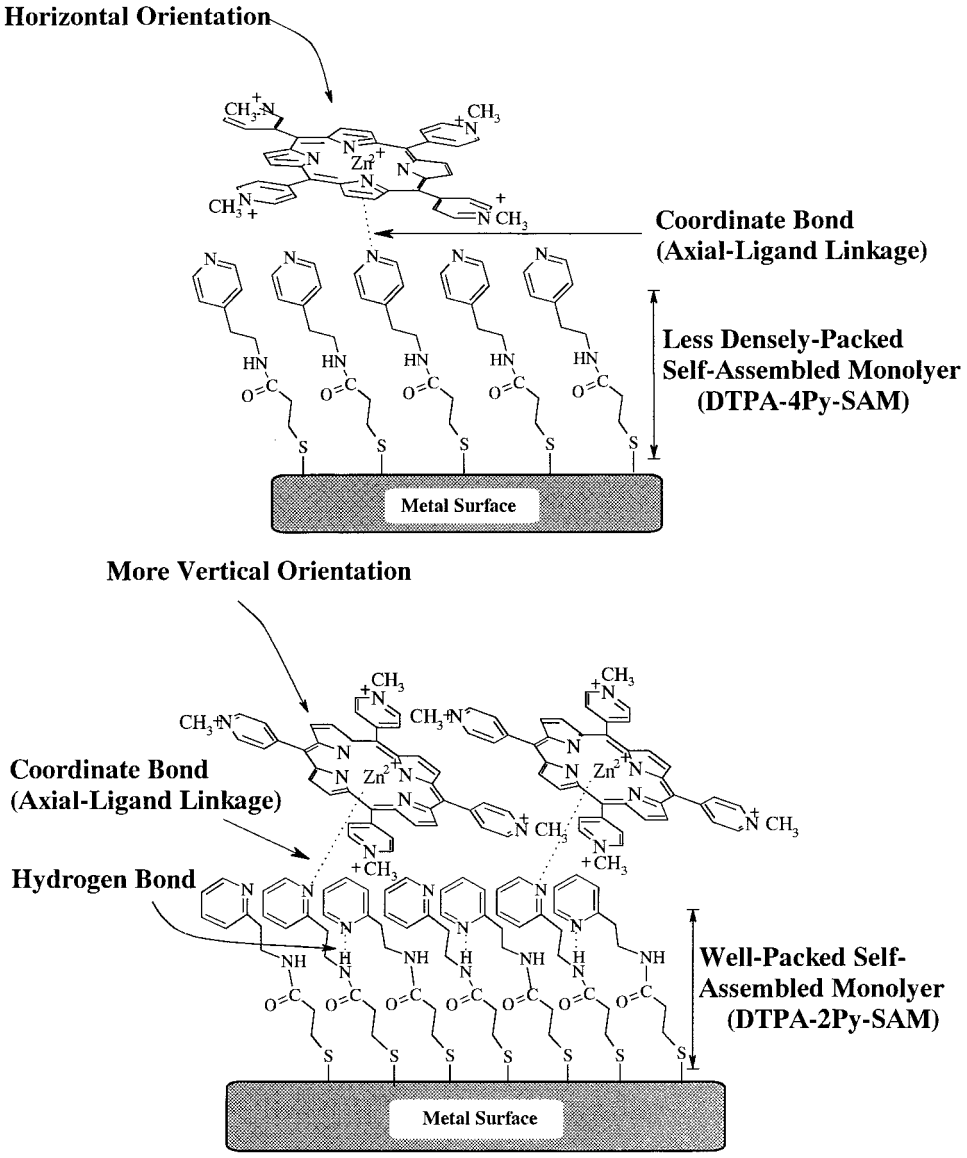

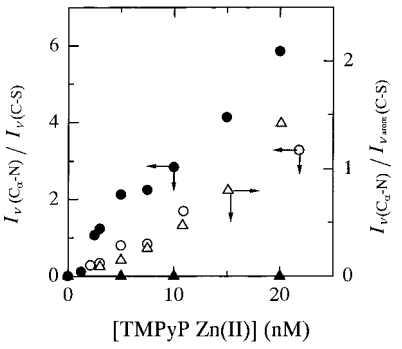

Figure 6. Concentration dependences of the relative intensity of $\nu(C_\alpha-N)$ for the porphyrin to that for $\nu(C-S)$ (or $\nu_{arom}(C-S)$) of various SAMs carrying pyridine ring moieties: ●, DTPA-2Py-SAM; ○, DTPA-4Py-SAM; △, 4Py-SAM; ▲, 2Py-SAM.

the concentration of porphyrin, the value of $(I_{\nu(C_\alpha-N)}/I_{\nu_{arom}(C-S)})$ increased correspondingly, which reflects the binding of the porphyrin to the DTPA-4Py-SAM.

In contrast to this, a unique relationship could be observed between the relative peak intensity of $\nu(C_\alpha\text{-}N)$ to that for $\nu_{arom}(C-S)$ of the 4PySSPy−silver colloid mixture (4-Py-SAM), which was incubated with various concentrations of TMPyP Zn(II) (Figure 6, open triangle). The ratio of relative intensities increased in an "accelerative" manner with the concentration of porphyrin. Though we have no definite explanation of this phenomenon at this moment, there is a possibility that, by the binding of the porphyrin molecules to the surface of 4Py-SAM, the stretching of $\nu_{arom}(C-S)$ was reduced, and consequently, the value of relative intensities $(I_{\nu(C_\alpha-N)}/I_{\nu_{arom}(C-S)})$ increased extensively: by the adsorption of porphyrin on the SAM surface, a pyridine−porphyrin complex was formed. As a result, the effective mass of the pyridine moiety might increase, and the stretching of the C−S bond might decrease. Consequently, the value of the relative intensities $(I_{\nu(C_\alpha-N)}/I_{\nu_{arom}(C-S)})$ would increase extensively.

In the case of DTPA-4Py-SAM, on the other hand, the distance between the pyridine ring and the C−S bond moiety is longer than that of 4Py-SAM, and therefore, the adsorption of the porphyrin molecules on the SAM surface might not affect the stretching of $\nu(C-S)$ significantly. Consequently, the relative intensity increased proportionally to the concentration of porphyrin added.

We tried to estimate the saturated amount of porphyrin, but above this concentration range (>22 nM), the intensity of resonance Raman scattering was not negligible, and therefore,

the estimation of the saturated amount of porphyrin on the surface of SAM was not possible at this moment.

(3) TMPyP Zn(II)/DTPA-2Py-SAM and 2Py-SAM Systems. Next, the effect of the position of the nitrogen atom in the pyridine ring on the binding of porphyrin to the SAM was examined. When the SAM prepared by the incubation of DTPA-2Py with the Ag colloid (DTPA-2Py-SAM) was further incubated with TMPyP Zn(II) for 30 min at room temperature, new bands (384, 798, 1250, and 1353 cm^{-1}) corresponding to the porphyrin appeared in a manner similar to the DTPA-4Py-SAM and 4Py-SAM systems. The relative peak intensity of $\nu(C_\alpha\text{-N})$ between the α-carbon and the nitrogen of pyrrole in the porphyrin at 1353 cm^{-1} to that for $\nu(C-S)$ (650 cm^{-1}) was plotted against the concentration of porphyrin added (Figure 6, filled circle). Compared with the DTPA-4Py-SAM, the Raman scattering corresponding to the porphyrin moiety of the DTPA-2Py-SAM was more clearly observed.

At the surface of DTPA-2Py-SAM, which had a smaller molecular surface area than DTPA-4Py-SAM, more pyridine rings exist in a unit area than in DTPA-4Py-SAM (Table 1) and therefore, more porphyrin molecules would be able to adsorb to the DTPA-2Py-SAM surface. In addition, the SER effect might act on the normal components more effectively than the tangential ones,[16a] because the normal electric field component is larger than the tangential one due to the presence of a surface plasmon.[16d,23] Taking account of this, it may be said that the orientation of porphyrin absorbed to the DTPA-2Py-SAM is somewhat more vertical than that absorbed to the DTPA-4Py-SAM, and therefore, the Raman scattering corresponding to the porphyrin was enhanced more effectively than that to the DTPA-4Py-SAM (Scheme 3).

Recently, it has been reported that the Γ value of TMPyP H_2 is 3.20 nm^2.[24] This value is much larger than those of the SAM-forming molecules examined here (0.27−0.41 nm^2, Table 1). Since TMPyP Zn(II) possesses the same molecular surface area as that of TMPyP H_2, it can be said that the orientation of the metalloporphyrin ring on the SAM surface would be more effective on the enhancement of the peak intensity for $\nu(C_\alpha-N)$ than the difference in the density of molecular packing in the SAMs discussed above.

Similarly, the interaction between 2Py-SAM and TMPyP Zn(II) was examined (Figure 6, filled triangle). There was no change in the Raman spectra of 2Py-SAM even in the presence of a high concentration of TMPyP Zn(II) (20 nM), which indicates the absence of porphyrin on the surface of SAM. These results suggest that the presence of the nitrogen atom at the exterior surface of SAM (i.e., the nitrogen atom of the pyridine ring is directed to the solution phase) is essential for the attachment of porphyrin to the SAM surface.

In the cases of DTPA-4Py-SAM, DTPA-2Py-SAM, and 4Py-SAM, the nitrogen atom in the pyridine ring can exist at the exterior of SAM as an axial ligand to bind the porphyrin ring in which a zinc ion was incorporated. In contrast, 2Py-SAM, which has a nitrogen atom in the interior of the SAM (i.e., the nitrogen atom of the pyridine ring is directed to the silver surface) cannot be an effective axial ligand due to the steric hindrance.

As discussed previously, the TMPyP Zn(II) attaches to the surface of the pyridine ring-carrying SAM via the coordinate bonding between the zinc ion in the core of porphyrin ring and the nitrogen atom of the pyridine ring and not by the nonspecific physical adsorption. The pyridine ring pursues a role as a specific axial ligand to be stacked by the porphyrin. The alkyl spacer between the pyridine ring and the disulfide group enables the pyridine ring on the SAM surface to act as a much more effective ligand, because the pyridine ring, which is more densely attached to the metal surface, orients more perpendicularly to the surface than without the spacer. Therefore, the difference between the relative intensities of $\nu(C_\alpha-N)$ for DTPA-2Py-SAM and 2Py-SAM in Figure 6 is understandable.

Acknowledgment. This work was supported by a Grant-in-Aid for Scientific Research on Priority Areas (10126221, 11167236) from the Ministry of Education, Science, Sports, and Culture. The authors are indebted to Rengo Co., Ltd., Osaka, Japan, for its financial support. This paper was presented at the 47th Regional Meeting of the Society of Polymer Science, Japan, in October, 1998, at Toyama University, Toyama, Japan.

References and Notes

(1) (a) Nuzzo, R. G.; Allara, D. L. *J. Am. Chem. Soc.* **1983**, *105*, 4481. (b) Nuzzo, R. G.; Fusco, F. A.; Allara, D. L. *J. Am. Chem. Soc.* **1987**, *109*, 2358. (c) Proter, M. D.; Bright, T. B.; Allara, D. L.; Chidsey, C. E. D. *J. Am. Chem. Soc.* **1987**, *109*, 3559. (d) Bain, C. D.; Troughton, E. B.; Tao, Y.-T.; Evall, J.; Whitesides, G. M.; Nuzzo, R. G. *J. Am. Chem. Soc.* **1989**, *111*, 321. (e) Bain, C. D.; Whitesides, G. M. *Adv. Mater.* **1989**, *1*, 506. (f) Chidsey, C. E. D.; Loiacono, D. N. *Langmuir* **1990**, *6*, 682. (g) Laibinis, P. E.; Whitesides, G. M.; Allara, D. L.; Yu-Tai Tao.; Parkih, A. N.; Nuzzo, R. G. *J. Am. Chem. Soc.* **1991**, *113*, 7152. (h) Dubois, L. H.; Nuzzo, R. G. *Annu. Rev. Phys. Chem.* **1992**, *43*, 437. (i) Hill, W.; Wehling, B. *J. Phys. Chem.* **1993**, *97*, 9451.

(2) (a) Troughton, E. B.; Bain, C. D.; Whitesides, G. M.; Allara, D. L.; Proper, M. D. *Langmuir* **1988**, *4*, 365. (b) Katz, E.; Itzhak, N.; Willner, I. *J. Electroanal. Chem.* **1992**, *336*, 357.

(3) (a) Spinke, J.; Lileym, M.; Gunder, H.-J.; Angermaier, L.; Knoll, W. *Langmuir* **1993**, *9*, 1821. (b) Prime, K. L.; Whitesides, G. M. *J. Am. Chem. Soc.* **1993**, *115*, 10714. (c) Lopez, G. P.; Albers, M. W.; Schreiber, S. L.; Carroll, R.; Peralta, E.; Whitesides, G. M. *J. Am. Chem. Soc.* **1993**, *115*, 5877. (d) Schönher, H.; Vancso, G. J.; Huisman, B.-H.; van Veggel, F. C. J. M.; Reinhoudt, D. N. *Langmuir* **1997**, *13*, 1567. (e) Schierbaum, K.-D.; Weiss, T.; van Velzen, E. U. T.; Engbersen, J. F. J.; Reinhoudt, D. N.; Göpel, W. *Science* **1994**, *265*, 1413. (f) Huisman, B.-H.; Kooyman, R. P. H.; van Veggel, F. C. J. M.; Reinhoudt, D. N. *Adv. Mater.* **1996**, *8*, 561. (g) Jeon, N. L.; Finnie, K.; Branshaw, K.; Nuzzo, R. G. *Langmuir* **1997**, *13*, 3382. (h) Flink, S.; Boukamp, B. A.; van den Berg, A.; van Veggel, F. C. J. M.; Reinhoudt, D. N. *J. Am. Chem. Soc.* **1998**, *120*, 4652. (i) Beulen, M. J.; Kastenberg, M. I.; van Veggel, F. C. J. M.; Reinhoudt, D. N. *Langmuir* **1998**, *14*, 7463. (j) Gorman, C. B.; Miller, R. L.; Chen, K.-Y.; Bishop, A. R.; Haasch, R. T.; Nuzzo, R. G. *Langmuir* **1998**, *14*, 3312.

(4) Maeda, Y.; Yamamoto, H.; Kitano, H. *J. Phys. Chem.* **1995**, *99*, 4837.

(5) Yoshizumi, A.; Kanayama, N.; Ide, M.; Kitano, H. *Langmuir* **1999**, *15*, 482.

(6) (a) Maeda, Y.; Kitano, H. *J. Phys. Chem.* **1995**, *99*, 487. (b) Yamamoto, H.; Maeda, Y.; Kitano, H. *J. Phys. Chem. B* **1997**, *101*, 6855. (c) Maeda, Y.; Fukuda, T.; Yamamoto, H.; Kitano, H. *Langmuir* **1997**, *13*, 4187. (d) Fukuda, T.; Maeda, Y.; Kitano, H. *Langmuir* **1999**, *15*, 1887. (e) Submitted.

(7) Kanayama, N.; Kitano, H. *Langmuir*, in press.

(8) Zak, J.; Yuan, H.; Ho, K.; Woo, L.; Porter, M. D. *Langmuir* **1993**, *9*, 2772.

(9) Hutchision, J. E.; Postlethwaite, T. A.; Murray, R. W. *Langmuir* **1993**, *9*, 3277.

(10) Offord, D. A.; Sachs, S. B.; Ennis, M. S.; Eberspacher, T. A.; Griffin, J. H.; Chidsey, C. E. D.; Collman, J. P. *J. Am. Chem. Soc.* **1998**, *120*, 4478−4487.

(11) (a) Kharlamov, B. M.; Personov, R. I.; Bykovskaya, L. A. *Opt. Commun.* **1974**, *12*, 191. (b) Gorokhovski, A. A.; Kaarli, R.; Rebane, L. A. *LETP Lett.* **1974**, *20*, 216. (c) Gorokhovski, A. A.; Kaarli, R.; Rebane, L. A. *Opt. Commun.* **1976**, *16*, 282. (d) Friedrich, J.; Haarmer, D. *Angew. Chem., Int. Ed. Engl.* **1984**, *23*, 113. (e) Kishi, N.; Asai, N.; Kawashima, K. *Appl. Phys. Lett.* **1988**, *52*, 16. (f) Carter, T. P.; Bräuchle, C.; Lee, V. Y. *J. Phys. Chem.* **1987**, *91*, 3998.

(12) (a) Nicolson, M. M.; Pizzarello, F. A. *J. Electrochem. Soc.* **1979**, *126*, 1490. (b) Nicolson, M. M.; Pizzarello, F. A. *J. Electrochem. Soc.* **1981**, *128*, 1740. (c) Yanagi, H.; Toriida, M. *J. Electrochem. Soc.* **1994**, *141*, 64.

(13) Blom, N.; Odo, J.; Nakamoto, K.; Strommen, D. P. *J. Phys. Chem.* **1986**, *90*, 2847.

(14) (a) Walczak, M. M.; Popenone, D. D.; Deinhammer, R. S.; Lamp, B. D.; Chung, C.; Porter, M. D. *Langmuir* **1991**, *7*, 2687. (b) Widrig, C. A.; Chung, C.; Porter, M. D. *J. Electroanal. Chem.* **1991**, *310*, 335. (c)

Zhong, C. J.; Porter, M. D. *J. Am. Chem. Soc.* **1994**, *116*, 11616. (d) Rojas, M. T.; Königer, R.; Stoddart, J. F.; Kaifer, A. E. *J. Am. Chem. Soc.* **1995**, *117*, 336.

(15) (a) Fleischmann, M.; Hendra, P. J.; McQuillan, A. J.; *Chem. Phys. Lett.* **1974**, *26*, 163. (b) Jeanmaire, D. L.; VanDuyne, R. P. *J. Electroanal. Chem.* **1977**, *84*, 1. (c) Albrecht, M. G.; Creighton, J. A. *J. Am. Chem. Soc.* **1977**, *99*, 5215.

(16) (a) Bryant, M. A.; Pemberton, J. E. *J. Am. Chem. Soc.* **1991**, *113*, 3629. (b) Bryant, M. A.; Pemberton, J. E. *J. Am. Chem. Soc.* **1991**, *113*, 8284. (c) Joo, T.; Kim, K.; Kim, M. S. *J. Phys. Chem.* **1986**, *90*, 5816. (d) Pemberton, J. E.; Bryant, M. A.; Sobocinski, R. L.; Joa, S. L. *J. Phys. Chem.* **1992**, *96*, 3776.

(17) Sawaguchi, T.; Mizutani, F.; Taniguchi, I. *Langmuir* **1998**, *14*, 3565.

(18) Taniguchi, I.; Yoshimoto, S.; Nishiyama, K. *Chem. Lett.* **1997**, 353.

(19) (a) Strong, L.; Whitesides, G. M. *Langmuir* **1988**, *4*, 546. (b) Chidsey, C. E. D.; Loiacono, D. N. *Langmuir* **1990**, *6*, 709. (c) Dubois, L. H.; Zegarski, B. R.; Nuzzo, R. G. *J. Chem. Phys.* **1993**, *98*, 678.

(20) Eleighton, T. E. *Proteins Structures and Molecular Properties*; W. H. Freeman and Co.: New York, 1993; p 293.

(21) (a) Lenk, T. J.; Hallmark, V. M.; Hoffmann, C. L.; Rabolt, J. F. *Langmuir* **1994**, *10*, 4610. (b) Tam-Chang, S. W.; Biebuyck, H. A.; Whitesides, G. M.; Jeon, N.; Nuzzo, R. G. *Langmuir* **1995**, *11*, 4371. (c) Clegg, R. S.; Hutchison, J. E. *Langmuir* **1996**, *12*, 5239. (d) Sabapathy, R. C.; Bhattacharyya, S.; Leavy, M. C.; Cleland, W. E., Jr.; Hussey, C. L. *Langmuir* **1998**, *14*, 124.

(22) Ulman, A. *J. Mater. Ed.* **1989**, *11*, 205.

(23) Creighton, J. A.; Clark, R. J. H.; Hester, R. E. *Spectroscopy of Surface*; John Wiley & Sons: New York, 1988.

(24) Pietro, I.; Camacho, L.; Martín, M. T. *Langmuir* **1998**, *14*, 1853.